Journal of Organometallic Chemistry, 376 (1989) 67–90
Elsevier Sequoia S.A., Lausanne – Printed in The Netherlands
JOM 20025

Nature of the hydrogen bridge in transition metal complexes

V *. Electronic structure of the carbonyl dimers with mixed bridges of the type $[(CO)_4M\begin{smallmatrix} \diagup H \diagdown \\ \diagdown L \diagup \end{smallmatrix}M(CO)_4]^n$

Bogusława Jeżowska-Trzebiatowska * **and Barbara Nissen-Sobocińska**
Institute for Low Temperature and Structure Research, Polish Academy of Sciences, Plac Katedralny 1, P.O. Box 937, 50-950 Wrocław (Poland)

Leszek Natkaniec
Institute of Chemistry, Wrocław University, F. Joliot-Curie 14, 50-383 Wrocław (Poland)

(Received April 19th, 1989)

Abstract

The electronic structure of the binuclear complexes having mixed double bridges, $[(CO)_4M\begin{smallmatrix} \diagup H \diagdown \\ \diagdown L \diagup \end{smallmatrix}M(CO)_4]^n$ where $M = Mo$, $L = H^-$, OH^-, Cl^-, PH_2^- and $n = -2$ or $M = Mn$, $L = PH_2^-$ and $n = 0$ has been calculated by use of the Fenske–Hall method. The results allowed the comparison of the roles played by the hydrogen atom and ligands L in the formation of the mixed double bridges. The character of the M–H–M and M–L–M bridge bonds is similar but the stability of the M–L–M is higher because of the greater delocalization of the atomic orbitals of L bridge ligand than of the H bridge ligand. The *trans* effect of the bridge hydrogen atom was characterized as being larger than the *trans* effect of L bridge ligand. The contribution of the 3*d* atomic orbitals of the phosphorus atom in the formation of the mixed bridges in complexes $[(CO)_4Mo\begin{smallmatrix} \diagup H \diagdown \\ \diagdown PH_2 \diagup \end{smallmatrix}Mo(CO)_4]^{-2}$ and $(CO)_4Mn\begin{smallmatrix} \diagup H \diagdown \\ \diagdown PH_2 \diagup \end{smallmatrix}Mn(CO)_4$ was discovered.

Introduction

Of the known transition metal complexes having M–H–M bridge bonds a large group comprises compounds having mixed bridges, i.e. those with the hydrogen

---

* For part IV see ref. 9.

Table 1

Bond lengths (Å) used in the calculations

Complex	M–M	M–H_B [a]	M–L_B [b]	M–C_I [c]	M–C_{II} [d]
$[(CO)_4Mo\overset{H}{\underset{H}{}}Mo(CO)_4]^{-2}$	3.267	1.86		1.96	1.96
$[(CO)_4Mo\overset{H}{\underset{Cl}{}}Mo(CO)_4]^{-2}$	3.267	1.86	2.477	1.96	1.96
$[(CO)_4Mo\overset{H}{\underset{PH_2}{}}Mo(CO)_4]^{-2}$	3.267	1.86	2.422	1.96	1.96
$[(CO)_4Mo\overset{H}{\underset{OH}{}}Mo(CO)_4]^{-2}$	3.267	1.86	2.08	1.96	1.96
$(CO)_4Mn\overset{H}{\underset{H}{}}Mn(CO)_4$	2.937	1.86		1.79	1.79
$(CO)_4Mn\overset{H}{\underset{PH_2}{}}Mn(CO)_4$	2.937	1.86	2.284	1.79	1.79

[a] H_B = bridge hydrogen atom. [b] L_B = bridge ligand. [c] C_I = carbon atom in perpendicular plane to bridge core. [d] C_{II} = carbon atom in bridge plane.

bridges supported by the other bridges. These complexes contain the various bridge cores, e.g. $M\overset{H}{\underset{L}{}}M$, $M\overset{H}{\underset{L}{-L-}}M$, $M\overset{H}{\underset{L}{-H-}}M$ [1]. Most of the complexes of this type are unstable intermediates in catalytic processes.

In previous reports, on the basis of the electronic structure calculations (by use of the Fenske–Hall method), we have discussed the role of the hydrogen atom and of other bridge ligands (such as Cl^- and CO) in the formation of the triple mixed bridges in the complexes $[L_3M\overset{H}{\underset{L}{-L-}}ML_3]^n$ and have compared the *trans* effect of the bridge ligands: H^-, Cl^-, and CO [2].

The role of the bridge ligands H^-, Cl^-, CO in complexes of that type has been found to be comparable. From a comparison of the electronic structures of $[L_3M\overset{L}{\underset{L}{-L-}}ML_3]^n$ and $[L_3M\overset{H}{\underset{L}{-L-}}ML_3]^n$, where $L = Cl^-, CO$, it follows that the molecular levels corresponding to the M–H–M bridge bond are in the same energy range as other molecular levels corresponding to the M–L–M bridge bonds. The electron density distribution for the M–H–M and M–L–M bridge bonds is also very similar. Our calculations also revealed the comparable *trans* effect of the bridge ligands H^-, Cl^-, and CO.

Our goal was to examine the double mixed bridges from the same view point. For the calculations we selected the $[(CO)_4M\overset{H}{\underset{H}{}}M(CO)_4]^n$ complexes, where M = Mo, $L = OH^-$, Cl^-, PH_2^-, and $n = -2$ or M = Mn, $L = PH_2^-$, and $n = 0$. In a previous paper we have discussed the structure of the carbonyl complexes with double hydrogen bridge of the $[(CO)_4M\overset{H}{\underset{H}{}}M(CO)_4]^n$ type [3].

The structural data for the calculations (Table 1) were based on crystallographic structures for: $Mo_2(\mu\text{-}H)(\mu\text{-}PMe_2)Cp_2(CO)_4$ [4], $Mn_2(\mu\text{-}H)(\mu\text{-}PPh_2)(CO)_8$ [5], $[Mo_2(\mu\text{-}H)(\mu\text{-}Cl)_2Cl_6]^{-3}$ [6], $Mo_2(\mu\text{-}H)(\mu\text{-}OH)(\mu\text{-}C_{10}H_8)Cp_2$ [7]. The calculations

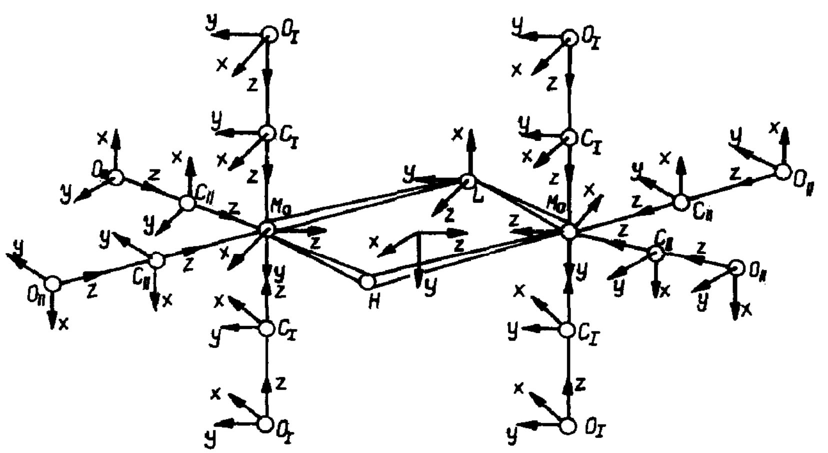

Fig. 1. Coordinate systems assumed in calculations for $[(CO)_4M\underset{H}{\overset{H}{\lessgtr}}M(CO)_4]^n$ and $[(CO)_4M\underset{L}{\overset{H}{\lessgtr}}M(CO)_4]^n$ complexes

were performed by the Fenske–Hall method [8]. The coordinate systems assumed in calculations are shown in Fig. 1.

Results and discussion

From our previous calculations for the carbonyl dimer of molybdenum $[(CO)_4Mo\underset{H}{\overset{H}{\lessgtr}}Mo(CO)_4]^{-2}$ (Fenske–Hall method), the atomic function basis for molybdenum has the valence functions $4d$, $5s$ and $5p$. However, in the calculations presented here, we have used a different atomic function basis for molybdenum, one that includes the $5d$ atomic orbitals of Mo, which has no influence on the electronic structure, because the $5d$ orbitals of Mo do not contribute to the formation of the occupied molecular levels, but the electron density distribution does change a little (Table 2).

The structure of the carbonyl dimer of molybdenum having a double hydrogen bridge could be characterized as follows (irrespective of the function basis used):

(1) the lowest levels of the exclusively σ MO's of the CO groups,

(2) intermixed levels of varying character:
  (a) levels of the exclusively σ MO's of the CO groups,
  (b) levels of the exclusively π^b MO's of the CO groups,
  (c) levels corresponding to the bonding interactions of the σ^b MO's from the CO groups with the d orbitals of the metal atoms viz., σ^b–dM interactions,
  (d) levels corresponding to the bonding interactions of the π^b MO's of the CO groups with the d orbitals of the metal atoms, viz., π^b–dM interactions,

(3) two levels ($9a_g$,$6b_{3u}$), mainly AO's of the bridging hydrogen atoms and metal atoms, which correspond to the M–H–M bridge bonds,

(4) the highest filled levels of the π^a MO's of the CO groups and the d orbitals of the metal atoms, which correspond to the $\pi^a \to d$M bonding interactions. The electronic structure of the terminal energy levels for $[(CO)_4Mo\underset{H}{\overset{H}{\lessgtr}}Mo(CO)_4]^{-2}$ is presented in Tables 3 and 11. Replacement of one of bridge hydrogen atoms by the

Table 2

Mulliken atomic charges and overlap populations for the complexes $[(CO)_4Mo\langle\begin{smallmatrix}H\\L\end{smallmatrix}\rangle Mo(CO)_4]^{-2}$

Charges and overlap populations	Calculation including the 5*d* AO's of Mo				Calculation excluding the 5*d* AO's of Mo	
	$[(CO)_4Mo\langle\begin{smallmatrix}H\\H\end{smallmatrix}\rangle Mo(CO)_4]^{-2}$	$[(CO)_4Mo\langle\begin{smallmatrix}H\\OH\end{smallmatrix}\rangle Mo(CO)_4]^{-2}$	$[(CO)_4Mo\langle\begin{smallmatrix}H\\Cl\end{smallmatrix}\rangle Mo(CO)_4]^{-2}$	$[(CO)_4Mo\langle\begin{smallmatrix}H\\PH_2\end{smallmatrix}\rangle Mo(CO)_4]^{-2}$ Calculation excluding 3*d* AO's of P	$[(CO)_4Mo\langle\begin{smallmatrix}H\\H\end{smallmatrix}\rangle Mo(CO)_4]^{-2}$	$[(CO)_4Mo\langle\begin{smallmatrix}H\\PH_2\end{smallmatrix}\rangle Mo(CO)_4]^{-2}$ Calculation including 3*d* AO's of P
Mo	1.243	1.190	1.124	1.003	0.746	0.559
H_B	−0.488	−0.491	−0.502	−0.499	−0.331	−0.266
L_B		OH −0.429	Cl −0.374	PH_2 −0.061		PH_2 −0.388
		O −0.612		P 0.017		P −0.362
		H 0.183		H −0.039		H −0.063
$CO^{II\,a}$	−0.474	-0.491^{c}	-0.487^{c}	0.475^{c}	−0.391	-0.348^{c}
		-0.451^{t}	-0.421^{t}	-0.436^{t}		-0.336^{t}
CO_I	−0.405	−0.394	−0.388	−0.272	−0.316	−0.274
Mo–Mo	−0.008	−0.015	−0.005	−0.006	0.023	−0.028
Mo–H_B	0.118	0.117	0.120	0.122	0.147	0.124
Mo–L_B		0.145	0.177	0.192		0.380
Mo–CO_{II} [b]	0.381	0.395^{c}	0.395^{c}	0.393^{c}	0.395	0.399^{c}
		0.383^{t}	0.377^{t}	0.376^{t}		0.385^{t}
Mo–CO_I	0.400	0.398	0.407	0.408	0.418	0.411
*d*Mo–CO_{II}	0.300	0.295^{c}	0.294^{c}	0.284^{c}	0.247	0.253^{c}
		0.286^{t}	0.285^{t}	0.275^{t}		0.236^{t}
*d*Mo–CO_I	0.264	0.259	0.266	0.264	0.222	0.210

[a,b] *c* values are related to carbonyl groups in the *cis* position to bridge hydrogen atom ($CO_{II}{}^{c}$), *t* values are related to carbonyl groups in the *trans* position to bridge hydrogen atom ($CO_{II}{}^{t}$)

Table 3

Energies and compositions of highest occupied molecular energy levels of $[(\mathrm{CO})_4\mathrm{Mo}\genfrac{}{}{0pt}{}{\mathrm{H}}{\mathrm{H}}\mathrm{Mo(CO)}_4]^{-2}$ with D_{2h} symmetry, calculation including the $5d$ AO's of Mo

Mo	Energy (eV)	Greatest contributions by the valence atomic orbitals (%)							
$11a_g$	−0.91	$p_y\mathrm{C_I}$	59	$p_y\mathrm{O_I}$	32	$s\mathrm{H_B}$	3		
$6b_{2g}$ LUMO	−1.52	$p_x\mathrm{C_I}$	48	$p_x\mathrm{O_I}$	28	$p_y\mathrm{C_{II}}$	8	$4d_{xz}\mathrm{Mo}$	7
$10a_g$ HOMO	−4.53	$p_y\mathrm{O_{II}}$	47	$p_y\mathrm{C_{II}}$	14	$4d_{z^2}\mathrm{Mo}$	11	$4d_{x^2-y^2}\mathrm{Mo}$	10
$9b_{1u}$	−4.70	$p_y\mathrm{O_{II}}$	55	$4d_{z^2}\mathrm{Mo}$	19	$p_y\mathrm{C_{II}}$	12	$4d_{x^2-y^2}\mathrm{Mo}$	10
$6b_{3g}$	−4.99	$p_y\mathrm{O_I}$	34	$4d_{yz}\mathrm{Mo}$	30	$p_x\mathrm{O_{II}}$	20	$p_y\mathrm{C_I}$	10
$3a_u$	−5.34	$p_x\mathrm{O_I}$	37	$4d_{xy}\mathrm{Mo}$	29	$p_x\mathrm{O_{II}}$	25	$p_x\mathrm{C_I}$	7
$3b_{1g}$	−5.40	$p_x\mathrm{O_I}$	38	$4d_{xy}\mathrm{Mo}$	29	$p_x\mathrm{O_{II}}$	25	$p_x\mathrm{C_I}$	7
$6b_{2u}$	−5.46	$p_y\mathrm{O_I}$	42	$4d_{yz}\mathrm{Mo}$	28	$p_x\mathrm{O_{II}}$	20	$p_y\mathrm{C_I}$	7
$6b_{3u}$	−6.30	$s\mathrm{H_B}$	56	$p_x\mathrm{Mo}$	9	$p_x\mathrm{O_I}$	8	$4d_{xz}\mathrm{Mo}$	5
$9a_g$	−7.74	$s\mathrm{H_B}$	54	$p_y\mathrm{O_{II}}$	14	$4d_{z^2}\mathrm{Mo}$	9	$p_y\mathrm{C_{II}}$	4
$5b_{2u}$	−8.06	$p_x\mathrm{O_{II}}$	49	$p_x\mathrm{C_{II}}$	13	$p_z\mathrm{C_I}$	9	$p_z\mathrm{O_I}$	4
$5b_{3g}$	−8.09	$p_x\mathrm{O_{II}}$	50	$p_x\mathrm{C_{II}}$	13	$p_z\mathrm{C_I}$	10	$p_y\mathrm{O_I}$	10

$\mathrm{C_I}$ = carbon atom of the CO group perpendicular to bridge plane, $\mathrm{O_I}$ = oxygen atom of the CO group perpendicular to bridge plane, $\mathrm{C_{II}}$ = carbon atom of the CO group in bridge plane, $\mathrm{O_{II}}$ = oxygen atom of the CO group in bridge plane, $\mathrm{H_B}$ = bridge hydrogen atom.

Table 4

Energies and compositions of the all occupied levels with participation of the AO's of bridge ligand L for the $[(\mathrm{CO})_4\mathrm{Mo}\overset{\mathrm{H}}{\underset{\mathrm{L}}{\lessgtr}}\mathrm{Mo}(\mathrm{CO})_4]^{-2}$ anions (Fig. 2)

MO	Energy (eV)	Greatest contributions by the valence atomic orbitals(%)							
$[(CO)_4Mo\overset{H}{\underset{OH}{\lessgtr}}Mo(CO)_4]^{-2}$									
$1a_1$	−30.53	$s\mathrm{O}_{\mathrm{OH}}$	77	$s\mathrm{H}_{\mathrm{OH}}$	23				
$6a_1$	−16.08	$s\mathrm{C}_{\mathrm{II}}$	31	$p_z\mathrm{O}_{\mathrm{OH}}$	21	$4d_{xz}\mathrm{Mo}$	19	$s\mathrm{O}_{\mathrm{OH}}$	7
$8a_1$	−14.25	$p_z\mathrm{O}_{\mathrm{OH}}$	35	$s\mathrm{C}_{\mathrm{I}}$	34	$p_z\mathrm{O}_{\mathrm{I}}$	13	$s\mathrm{O}_{\mathrm{OH}}$	6
$7b_1$	−11.46	$p_z\mathrm{O}_{\mathrm{I}}$	36	$p_y\mathrm{O}_{\mathrm{OH}}$	15	$p_z\mathrm{C}_{\mathrm{I}}$	13	$\mathrm{p}_z\mathrm{O}_{\mathrm{I}}$	10
$8b_1$	−11.10	$p_z\mathrm{C}_{\mathrm{I}}$	22	$p_z\mathrm{O}_{\mathrm{I}}$	19	$p_y\mathrm{O}_{\mathrm{OH}}$	18	$4d_{xz}\mathrm{Mo}$	8
$9b_1$	−10.42	$p_z\mathrm{O}_{\mathrm{II}}$	49	$p_z\mathrm{C}_{\mathrm{II}}$	25	$s\mathrm{Mo}$	4	$p_y\mathrm{O}_{\mathrm{OH}}$	2
$13b_1$	−8.46	$p_y\mathrm{O}_{\mathrm{II}}$	22	$p_y\mathrm{O}_{\mathrm{OH}}$	17	$p_x\mathrm{O}_{\mathrm{I}}$	14	$p_y\mathrm{C}_{\mathrm{II}}$	14
$7b_2$	−8.27	$p_x\mathrm{O}_{\mathrm{OH}}$	39	$p_y\mathrm{O}_{\mathrm{I}}$	27	$p_x\mathrm{O}_{\mathrm{I}}$	13	$p_x\mathrm{O}_{\mathrm{I}}$	8
$14b_1$	−8.14	$p_y\mathrm{O}_{\mathrm{II}}$	51	$p_y\mathrm{C}_{\mathrm{II}}$	17	$p_y\mathrm{O}_{\mathrm{OH}}$	12	$p_z\mathrm{C}_{\mathrm{II}}$	4
$8b_2$	−7.85	$p_x\mathrm{O}_{\mathrm{II}}$	46	$p_x\mathrm{O}_{\mathrm{OH}}$	21	$p_x\mathrm{C}_{\mathrm{II}}$	12	$p_z\mathrm{C}_{\mathrm{I}}$	7
$10b_2$	−4.57	$p_y\mathrm{O}_{\mathrm{I}}$	18	$p_x\mathrm{O}_{\mathrm{II}}$	18	$p_x\mathrm{O}_{\mathrm{OH}}$	17	$4d_{yz}\mathrm{Mo}$	11
$[(CO)_4Mo\overset{H}{\underset{Cl}{\lessgtr}}Mo(CO)_4]^{-2}$									
$4a_1$	−24.04	$s\mathrm{Cl}$	97	$4d_{xz}\mathrm{Mo}$	3				
$8b_1$	−10.96	$p_z\mathrm{O}_{\mathrm{II}}$	28	$p_y\mathrm{Cl}$	22	$p_y\mathrm{C}_{\mathrm{II}}$	12	$4d_{xz}\mathrm{Mo}$	11

$10a_1$	−10.64	p_zO_{II}	30	p_zCl	13	p_yC_{II}	10	p_zC_{II}	10
$9b_1$	−10.61	p_zO_{II}	38	p_zC_{II}	20	p_yCl	9	sMo	5
$12a_1$	−9.40	p_yO_I	51	p_yC_I	33	p_zCl	8	sH_B	2
$13a_1$	−9.32	p_xC_I	34	p_xO_I	55	p_zCl	5	sH_B	2
$14a_1$	−8.45	p_yO_{II}	25	p_zCl	20	p_yC_{II}	19	p_yO_{II}	16
$13b_1$	−8.39	p_yO_{II}	43	p_yC_{II}	26	p_yO_{II}	10	p_yCl	7
$7b_2$	−8.19	p_xCl	23	p_yO_I	22	p_xO_{II}	17	p_xC_{II}	7
$15a_1$	−8.15	p_zCl	30	p_yO_{II}	25	p_yC_{II}	13	sH_B	5
$14b_1$	−8.05	p_yCl	33	p_yO_{II}	32	p_yC_{II}	5	p_yO_I	5
$8b_2$	−7.82	p_xCl	46	p_xO_{II}	29	p_xC_{II}	9	p_zC_I	4
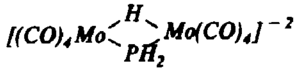 $[(CO)_4Mo\underset{PH_2}{\overset{H}{\lessgtr}}Mo(CO)_4]^{-2}$ (calculation excluding $3d$ AO's of P)									
$4a_1$	−20.45	sP	69	sH_{PH_2}	36				
$2b_2$	−14.94	sH_{PH_2}	42	p_xP	38	sC_I	11	p_zC_I	5
$3b_2$	−14.74	sC_I	32	p_zO_I	23	sH_{PH_2}	10	p_xP	8
$9a_1$	−11.04	p_zO_{II}	35	p_zP	18	$4d_{xz}$Mo	16	p_zC_{II}	9
$9b_1$	−10.34	p_yC_{II}	22	p_yP	15	p_zO_{II}	15	p_yO_{II}	11
$11a_1$	−9.87	p_yC_{II}	40	p_yO_{II}	31	p_zP	4	$4d_{z^2}$Mo	4
$15a_1$	−8.02	p_yO_{II}	43	p_yC_{II}	16	p_zP	8	p_yO_I	8
$14b_1$	−6.80	p_yP	41	p_yO_{II}	25	p_yO_{II}	5	p_zC_{II}	3
$15b_1$	−3.81	p_yO_{II}	37	$4d_{z^2}$Mo	17	p_yC_{II}	15	p_yP	11

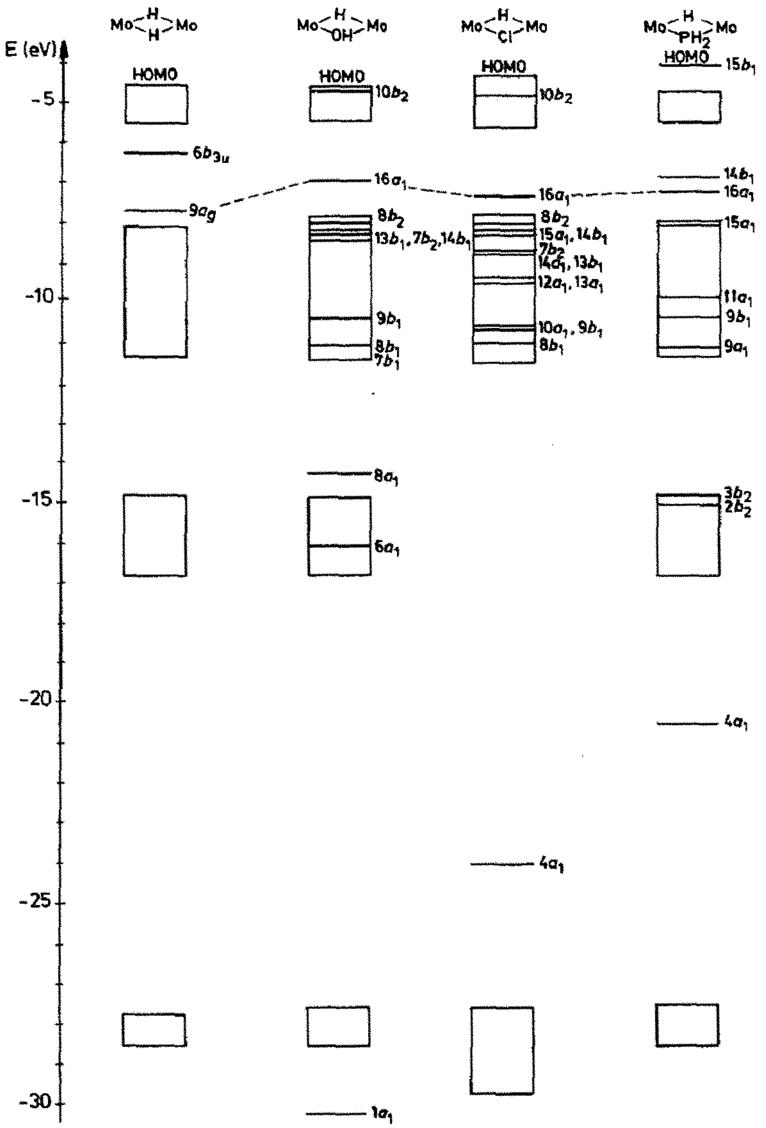

Fig. 2. Electronic structure of the $[(CO)_4Mo\overset{H}{\underset{L}{\langle\rangle}}Mo(CO)_4]^{-2}$ anions (calculation including the 5*d* AO's of Mo atoms) showing all bridge levels

ligand L in that anion causes no changes in the lower energy levels corresponding to the σ or π molecular orbitals of the CO groups or to the σCO–*d*M and π^bCO–*d*M interactions. In the energy range corresponding to these energy levels, are also present levels of considerably high contribution of the atomic orbitals of the bridge ligand: $1a_1$, $6a_1$, $10a_1$, $9b_1$, $13b_1$, $7b_2$, $14b_1$, $8b_2$, $10b_2$ for $[(CO)_4Mo\overset{H}{\underset{OH}{\langle\rangle}}Mo(CO)_4]^{-2}$, $4a_1$, $8b_1$, $10a_1$, $9b_1$, $15a_1$, $14b_1$, $8b_2$, $10b_2$ for $[(CO)_4Mo\overset{H}{\underset{Cl}{\langle\rangle}}Mo(CO)_4]^{-2}$, and $4a_1$, $2b_2$, $3b_2$, $9a_1$, $9b_1$, $15a_1$, $14b_1$, $15b_1$ for $[(CO)_4Mo\overset{H}{\underset{PH_2}{\langle\rangle}}Mo$-

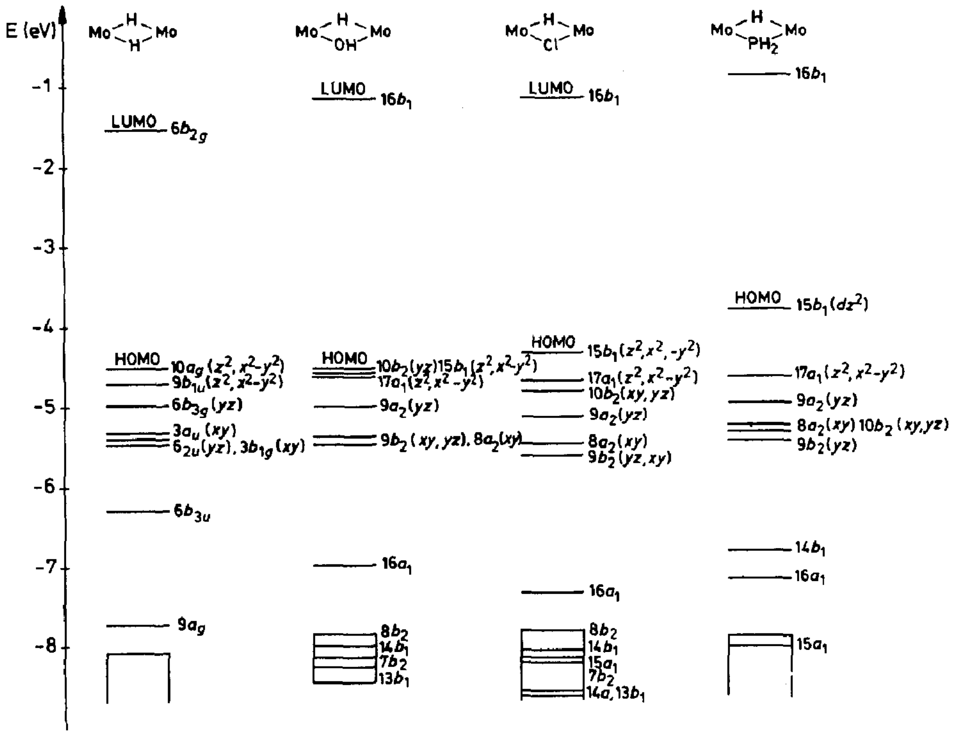

Fig. 3. Highest occupied molecular levels of the $[(CO)_4Mo\overset{H}{\underset{L}{\lessgtr}}Mo(CO)_4]^{-2}$ anions

$(CO)_4]^{-2}$ (Table 4 and Fig. 2). Some of these levels also have the character of metal atoms and could be regarded as corresponding to the M–L–M bridge bonds.

The last occupied molecular levels for all studied complexes are shown in Fig. 3. It is characteristic that the energy and the percent composition of one of the bridge levels ($9a_g$) does ot change on going from the double hydrogen bridge to the double mixed bridge. In $[(CO)_4Mo\overset{H}{\underset{L}{\lessgtr}}Mo(CO)_4]^{-2}$ the $16a$, level is related to the $9a_g$ energy level. The second, lower bridge level in $[(CO)_4Mo\overset{H}{\underset{H}{\lessgtr}}Mo(CO)_4]^{-2}$, $6b_{3u}$, is replaced by levels corresponding to the M–L–M bridge bonds.

Thus, the bridge ligand L orbitals are more delocalized than the 1*s* H orbital, which is why the M–L–M is more delocalized than the M–H–M bridge levels (Figs. 2 and 3). Moreover, for all the systems examined these levels are located mainly below the $16a_1$ level, but in each case a M–L–M bridge level exists of energy that exceeds the $16a_1$ level, namely: $10b_2$ for $[(CO)_4Mo\overset{H}{\underset{OH}{\lessgtr}}Mo(CO)_4]^{-2}$ and $[(CO)_4Mo\overset{H}{\underset{Cl}{\lessgtr}}Mo(CO)_4]^{-2}$, $14b_1$ and $15b_1$ for $[(CO)_4Mo\overset{H}{\underset{PH_2}{\lessgtr}}Mo(CO)_4]^{-2}$. This is why the complex with a double mixed bridge $[(CO)_4Mo\overset{H}{\underset{L}{\lessgtr}}Mo(CO)_4]^{-2}$ is more stable than $[(CO)_4Mo\overset{H}{\underset{H}{\lessgtr}}Mo(CO)_4]^{-2}$, the M–L–M bond is more stable than M–H–M in $[(CO)_4Mo\overset{H}{\underset{L}{\lessgtr}}Mo(CO)_4]^{-2}$ but to excite the M–L–M bonds requires very little energy.

Table 5

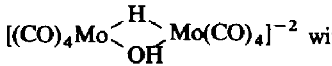

Energies and compositions of highest occupied molecular energy levels of $[(CO)_4Mo\underset{OH}{\overset{H}{\rightleftarrows}}Mo(CO)_4]^{-2}$ with C_{2v} symmetry, calculation including $5d$ AO's of Mo

Mo	Energy (eV)	Greatest contributions by the valence atomic orbitals (%)							
$18a_1$	−1.08	p_yC_{II}	50	p_yO_{II}	28	p_xC_I	12	p_xO_I	6
$16b_1$LUMO	−1.17	p_xC_I	48	p_xO_I	25	p_yC_I	7	p_yC_I	5
$15b_1$HOMO	−4.56	p_yO_{II}	54	$4d_{z^2}$Mo	21	p_yC_{II}	12	$4d_{x^2-y^2}$Mo	10
$10b_2$	−4.57	p_yO_I	18	p_xO_{II}	18	p_xO_{OH} [a]	17	$4d_{xz}$Mo	11
$17a_1$	−4.61	p_yO_{II}	49	$4d_{z^2}$Mo	14	$4d_{x^2-y^2}$Mo	10	p_yC_{II}	12
$9a_2$	−5.03	p_yO_I	34	$4d_{yz}$Mo	29	p_xO_{II}	20	p_yC_I	10
$8a_2$	−5.38	p_xO_{II}	35	$4d_{xy}$Mo	29	p_xO_{II}	26	p_xC_I	7
$9b_2$	−5.48	p_xO_{II}	23	p_xO_I	23	$4d_{xy}$Mo	18	$4d_{yz}$Mo	11
$16a_1$	−6.99	sH_B	53	p_yO_{II}	10	$4d_{z^2}$Mo	7	p_zC_I	6
$8b_2$	−7.85	p_xO_{II}	46	p_xO_{OH}	21	p_xC_{II}	12	p_zC_I	7
$7a_2$	−8.00	p_xO_{II}	50	p_xC_{II}	16	p_yO_I	11	p_yMo	1

[a] O_{OH} = oxygen atom of the OH group

Table 6

Energies and compositions of highest occupied molecular energy levels of 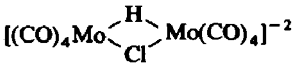 $[(\mathrm{CO})_4\mathrm{Mo}\begin{smallmatrix}\mathrm{H}\\ \mathrm{Cl}\end{smallmatrix}\mathrm{Mo}(\mathrm{CO})_4]^{-2}$ with C_{2v} symmetry, calculation including the 5*d* AO's of Mo

MO	Energy (eV)	Greatest contributions by the valence atomic orbitals (%)							
$18a_1$	−1.10	p_yC_I	57	p_yO_I	31	p_xC_I	4	p_xO_I	2
$16b_1$LUMO	−1.19	p_xC_{II}	47	p_xO_{II}	25	p_xC_I	9	p_xO_I	4
$15b_1$HOMO	−4.34	p_yO_{II}	48	$4d_{z^2}Mo$	19	p_yC_{II}	14	$4d_{x^2-y^2}Mo$	8
$17a_1$	−4.71	p_yO_{II}	38	p_yC_{II}	11	$4d_{z^2}Mo$	15	$4d_{x^2-y^2}Mo$	11
$10b_2$	−4.82	p_xO_{II}	20	p_xCl	18	$4d_{xy}Mo$	12	$4d_{yz}Mo$	10
$9a_2$	−5.14	p_yO_I	32	$4d_{yz}Mo$	29	p_xO_{II}	15	p_yC_I	9
$8a_2$	−5.49	p_xO_I	35	$4d_{xy}Mo$	28	p_xO_{II}	25	p_xC_I	7
$9b_2$	−5.63	p_xO_{II}	22	p_xO_I	18	$4d_{yz}Mo$	15	$4d_{xy}Mo$	13
$16a_1$	−7.33	sH_B	49	p_xO_I	6	p_zC_{II}	5	p_zCl	4
$8b_2$	−7.82	p_xCl	46	p_xO_{II}	29	p_xC_{II}	9	p_zC_I	4
$14b_1$	−8.05	p_yCl	33	p_yO_{II}	32	p_yC_{II}	5	p_yO_I	5
$7a_2$	−8.06	p_xO_{II}	42	p_xC_{II}	16	p_yO_I	10	p_xO_{II}	8

Table 7

Energies and compositions of highest occupied molecular energy levels of 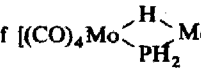 $[(CO)_4Mo\langle^{H}_{PH_2}\rangle Mo(CO)_4]^{-2}$, calculation excluding the 3*d* AOs of P and including 5*d* AO's of Mo (C_{2v} symmetry)

MO	Energy (eV)	Greatest contributions of the valence atomic orbitals (%)							
$18a_1$	−0.84	p_yC_I	57	p_yO_I	31	sH_B	3	p_xC_I	2
$16b_1$LUMO	−0.90	p_xC_I	32	p_yC_I	24	p_xO_I	16	p_yC_I	12
$15b_1$HOMO	−3.81	p_yO_{II}	37	$4d_{z^2}Mo$	17	p_yC_{II}	15	p_yP	11
$17a_1$	−4.63	p_yO_{II}	47	$4d_{z^2}Mo$	15	$4d_{x^2-y^2}Mo$	10	p_yC_{II}	10
$9a_2$	−4.97	p_yO_I	32	$4d_{yz}Mo$	29	p_xO_{II}	16	p_yC_I	9
$10b_2$	−5.25	p_xO_I	24	p_xO_{II}	23	$4d_{xy}Mo$	20	$4d_{yz}Mo$	9
$8a_2$	−5.32	p_xO_I	34	$4d_{xy}Mo$	28	p_xO_{II}	24	p_xC_I	7
$9b_2$	−5.46	p_yO_I	29	p_xO_{II}	20	$4d_{yz}Mo$	20	p_xO_I	13
$14b_1$	−6.80	p_yP	41	p_yO_{II}	25	p_yO_{II}	5	p_zC_{II}	3
$16a_1$	−7.18	sH_B	51	p_yO_{II}	12	$4d_{z^2}Mo$	8	p_xO_I	6
$7a_2$	−7.89	p_xO_{II}	49	p_xC_{II}	17	p_yO_I	10	p_xO_I	6

The effect of replacement of the bridge hydrogen atom by the ligand L on levels corresponding to the $d\mathrm{M}\rightarrow\pi^*\mathrm{CO}$ interactions is shown in Fig. 3. The energy levels do not change significantly; only the 4*d* AO's of Mo become more delocalized, because the anion symmetry is lowered (Tables 5,6,7). The energy of the HOMO levels for $[(\mathrm{CO})_4\mathrm{Mo}\underset{\mathrm{H}}{\overset{\mathrm{H}}{\lessgtr}}\mathrm{Mo}(\mathrm{CO})_4]^{-2}$, $[(\mathrm{CO})_4\mathrm{Mo}\underset{\mathrm{OH}}{\overset{\mathrm{H}}{\lessgtr}}\mathrm{Mo}(\mathrm{CO})_4]^{-2}$ and $[(\mathrm{CO})_4\mathrm{Mo}\underset{\mathrm{Cl}}{\overset{\mathrm{H}}{\lessgtr}}\mathrm{Mo}(\mathrm{CO})_4]^{-2}$ are comparable, whereas it is much higher for $[(\mathrm{CO})_4\mathrm{Mo}\underset{\mathrm{PH_2}}{\overset{\mathrm{H}}{\lessgtr}}\mathrm{Mo}(\mathrm{CO})_4]^{-2}$. The replacement of one of the hydrogen bridge atoms in the carbonyl manganese dimer $(\mathrm{CO})_4\mathrm{Mn}\underset{\mathrm{H}}{\overset{\mathrm{H}}{\lessgtr}}\mathrm{Mn}(\mathrm{CO})_4$ by a $\mathrm{PH_2}$ group is followed by destabilization of the HOMO and the other highest occupied levels (Figs. 4, 5 and Tables 8, 9).

In our first set of calculations we neglected to include the 3*d* AO's of phosphorus atom, which, could have been essential in the formation of the M–P–M type bonds. Inclusion of the 3d AO's of the P atom results in stabilization of the last filled levels for $[(\mathrm{CO})_4\mathrm{Mo}\underset{\mathrm{PH_2}}{\overset{\mathrm{H}}{\lessgtr}}\mathrm{Mo}(\mathrm{CO})_4]^{-2}$ and $(\mathrm{CO})_4\mathrm{Mn}\underset{\mathrm{PH_2}}{\overset{\mathrm{H}}{\lessgtr}}\mathrm{Mn}(\mathrm{CO})_4$. Only the levels

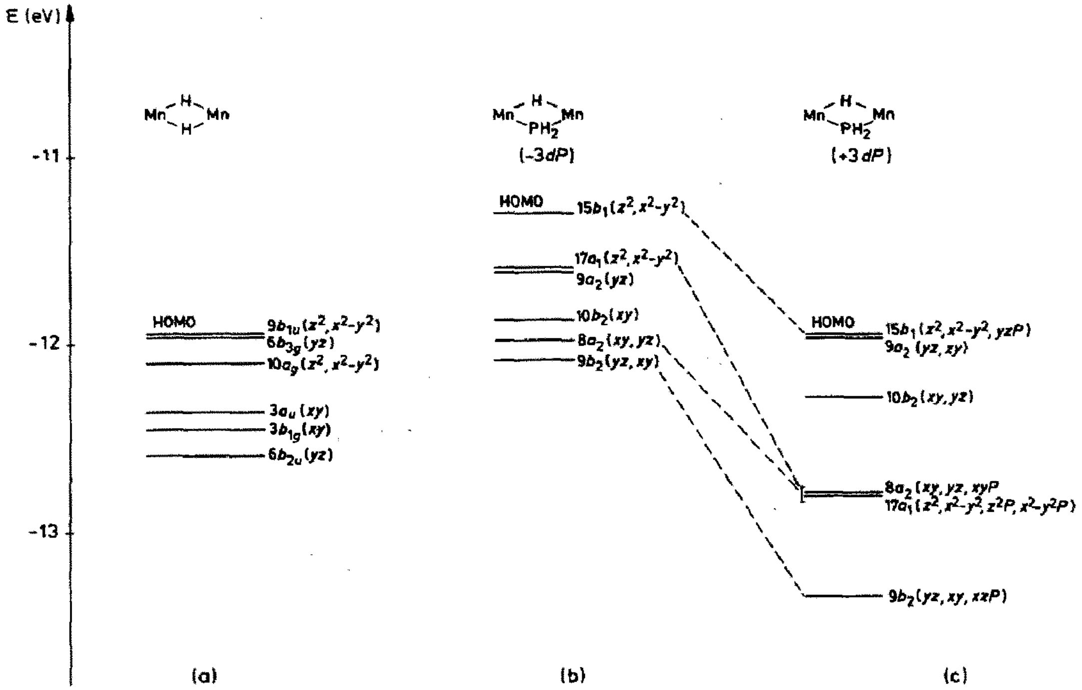

Fig. 4. Highest occupied molecular levels with much participation of 3d AO's of Mn (corresponding to $3d\mathrm{Mn}\rightarrow\pi^*\mathrm{CO}$ interactions) for: (a) $(\mathrm{CO})_4\mathrm{Mn}\underset{\mathrm{H}}{\overset{\mathrm{H}}{\lessgtr}}\mathrm{Mn}(\mathrm{CO})_4$, (b) $(\mathrm{CO})_4\mathrm{Mn}\underset{\mathrm{PH_2}}{\overset{\mathrm{H}}{\lessgtr}}\mathrm{Mn}(\mathrm{CO})_4$ calculation including the 3*d* AO's of P atom, (c) $(\mathrm{CO})_4\mathrm{Mn}\underset{\mathrm{PH_2}}{\overset{\mathrm{H}}{\lessgtr}}\mathrm{Mn}(\mathrm{CO})_4$ calculation excluding the 3*d* AO's of P atom.

Table 8

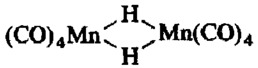

Energies and compositions of highest occupied molecular energy levels of $(\mathrm{CO})_4\mathrm{Mn}\genfrac{}{}{0pt}{}{\diagup\mathrm{H}\diagdown}{\diagdown\mathrm{H}\diagup}\mathrm{Mn}(\mathrm{CO})_4$ with D_{2h} symmetry

MO	Energy (eV)	Greatest contributions of the valence atomic orbitals (%)							
$10b_{1u}$	−5.29	$3d_{z^2}$Mn	38	p_yC$_{\mathrm{I}}$	16	p_zMn	14	p_yO$_{\mathrm{I}}$	10
$6b_{2g}$ LUMO	−9.60	$3d_{xz}$Mn	45	p_xMn	18	p_yO$_{\mathrm{II}}$	15	p_yC$_{\mathrm{II}}$	11
$9b_{1u}$ HOMO	−11.94	p_yO$_{\mathrm{I}}$	40	$3d_{z^2}$Mn	33	$3d_{x^2-y^2}$Mn	15	p_yC$_{\mathrm{II}}$	8
$6b_{3g}$	−11.98	$3d_{yz}$Mn	64	p_xO$_{\mathrm{II}}$	17	p_yO$_{\mathrm{I}}$	12	p_yC$_{\mathrm{I}}$	5
$10a_g$	−12.10	p_yC$_{\mathrm{II}}$	40	$3d_{z^2}$Mn	34	$3d_{x^2-y^2}$Mn	13	p_yC$_{\mathrm{II}}$	6
$3a_u$	−12.39	$3d_{xy}$Mn	56	p_xO$_{\mathrm{II}}$	24	p_xO$_{\mathrm{I}}$	12	p_xC$_{\mathrm{I}}$	5
$3b_{1g}$	−12.45	$3d_{xy}$Mn	55	p_xO$_{\mathrm{II}}$	24	p_xO$_{\mathrm{I}}$	12	p_xC$_{\mathrm{I}}$	6
$6b_{2u}$	−12.58	$3d_{yz}$Mn	57	p_xO$_{\mathrm{II}}$	20	p_yO$_{\mathrm{I}}$	14	p_yC$_{\mathrm{I}}$	7
$6b_{3u}$	−14.69	sH$_{\mathrm{B}}$	51	p_xMn	15	$3d_{xz}$Mn	13	p_yO$_{\mathrm{II}}$	12
$9a_g$	−14.74	sH$_{\mathrm{B}}$	58	p_zMn	19	$3d_{z^2}$Mn	13	p_yO$_{\mathrm{I}}$	4
$5b_{3g}$	−16.48	p_xO$_{\mathrm{II}}$	59	p_xC$_{\mathrm{II}}$	22	$3d_{yz}$Mn	3	p_yMn	3

Table 9

Energies and compositions of highest occupied molecular energy levels of $(\mathrm{CO})_4\mathrm{Mn}\genfrac{}{}{0pt}{}{\diagup\mathrm{H}\diagdown}{\diagdown\mathrm{PH_2}\diagup}\mathrm{Mn}(\mathrm{CO})_4$ with C_{2v} symmetry, calculation excluding the 3*d* AO's of P atom

MO	Energy (eV)	Greatest contributions of the valence atomic orbitals (%)							
$18a_1$	−3.73	$p_y\mathrm{C_{II}}$	55	$p_y\mathrm{O_{II}}$	24	$s\mathrm{H_B}$	9	$p_y\mathrm{C_I}$	4
$16b_1$ LUMO	−7.79	$3d_{z^2}\mathrm{Mn}$	30	$3d_{xz}\mathrm{Mn}$	15	$p_z\mathrm{Mn}$	7	$p_y\mathrm{O_I}$	6
$15b_1$ HOMO	−11.30	$3d_{z^2}\mathrm{Mn}$	34	$3d_{x^2-y^2}\mathrm{Mn}$	13	$p_y\mathrm{C_{II}}$	8	$3d_{xz}\mathrm{Mn}$	7
$17a_1$	−11.59	$3d_{z^2}\mathrm{Mn}$	36	$p_y\mathrm{O_{II}}$	36	$3d_{x^2-y^2}\mathrm{Mn}$	15	$p_y\mathrm{C_{II}}$	8
$9a_2$	−11.59	$3d_{yz}\mathrm{Mn}$	63	$p_x\mathrm{O_{II}}$	16	$p_y\mathrm{O_I}$	11	$p_y\mathrm{C_I}$	5
$10b_2$	−11.86	$3d_{xy}\mathrm{Mn}$	46	$p_x\mathrm{O_{II}}$	18	$3d_{yz}\mathrm{Mn}$	11	$p_x\mathrm{O_{II}}$	18
$8a_2$	−11.97	$3d_{xy}\mathrm{Mn}$	55	$p_x\mathrm{O_{II}}$	18	$3d_{yz}\mathrm{Mn}$	11	$p_y\mathrm{O_I}$	10
$9b_2$	−12.16	$3d_{yz}\mathrm{Mn}$	46	$p_x\mathrm{O_{II}}$	19	$3d_{xy}\mathrm{Mn}$	11	$p_y\mathrm{O_I}$	10
$16a_1$	−14.56	$s\mathrm{H_B}$	51	$3d_{xz}\mathrm{Mn}$	15	$p_x\mathrm{Mn}$	11	$p_y\mathrm{O_{II}}$	11
$14b_1$	−15.49	$p_y\mathrm{O_{II}}$	43	$p_y\mathrm{P_{II}}$	18	$3d_{xz}\mathrm{Mn}$	10	$p_z\mathrm{Mn}$	6
$8b_2$	−16.12	$p_x\mathrm{O_{II}}$	58	$p_x\mathrm{C_{II}}$	26	$3d_{yz}\mathrm{Mn}$	3	$p_y\mathrm{Mn}$	2
$7a_2$	−16.16	$p_x\mathrm{O_{II}}$	60	$p_x\mathrm{C_{II}}$	27	$3d_{yz}\mathrm{Mn}$	3	$p_y\mathrm{Mn}$	1

with contribution of the $3d$ AO's of P are lowered (Figs. 4, 5, 6, Tables 8, 9, 10 and 11, 12). The energy of the HOMO level in $(CO)_4Mn\overset{H}{\underset{PH_2}{\lessgtr}}Mn(CO)_4$ approaches the relevant values of a dimer having a double hydrogen bridge (Fig. 4). Moreover, the contribution of the $3d$ AO's of the P atoms to the formation of the bridge bond is responsible for the stabilization of $14b_1$ level vs. $16a_1$ level for $[(CO)_4Mo\overset{H}{\underset{PH_2}{\lessgtr}}Mo(CO)_4]^{-2}$ (Fig. 6).

The Mulliken population analysis reveals that on going from the carbonyl dimer with a $M\overset{H}{\underset{H}{\lessgtr}}M$ core to the dimer with a $M\overset{H}{\underset{L}{\lessgtr}}M$ core neither the overlap population $M{-}H_B$ nor a charge on the bridge hydrogen atom do not change, which corresponds to very small changes of energy and of the percent compositions of the $9a_g$ level. The decrease in the positive charge on the Mo atoms is proportional to the difference between charges on the bridge ligand L and on the hydrogen atom. The change in charge for the Mn atoms is much greater. The shift in the electron density with a change of a bridge ligand L mainly for metal atoms and the bridge ligand L, almost without participation of the bridge hydrogen atom, could be indicative for the the high stability of the M–H–M bridge bond (Tables 2, 13). It should be emphasized that in a dimer having a mixed bridge the negative charge on the bridge hydrogen atom exceeds only slightly that on the bridge ligand L (Table 2). An exception is the bridge PH_2 group for which in the first set of calculations (that excluded the $3d$ AO's of P) we obtained a value close to zero (-0.061) for the molybdenum dimer, and a positive value (0.553) for the manganese. However, if an acceptor character of the PH_2 group is assumed and the $3d$ AO's of the P atom are included in the calculations we obtained more similar negative charges on the bridge hydrogen atom (-0.266) and PH_2 group (-0.388) in $[(CO)_4Mo\overset{H}{\underset{PH_2}{\lessgtr}}Mo(CO)_4]^{-2}$ (Table 2). In the case of $(CO)_4Mn\overset{H}{\underset{PH_2}{\lessgtr}}Mn(CO)_4$ (Table 13) the inclusion of the $3d$ AO's of P atom results in a large change in charge on PH_2, from a positive value to close to zero (-0.004).

As in the complex with the double hydrogen bridge, at the same length assumed for all M–C bonds, in $[(CO)_4M\overset{H}{\underset{L}{\lessgtr}}M(CO)_4]^n$ the population analysis revealed a higher negative charge on the CO group in the bridge plane (CO_{II}) and a greater overlap population between d orbitals of the M atom and all orbitals of C atom of the CO_{II} group ($dM{-}C_{II}$) than adequate values for CO groups perpendicular to bridge plane (CO_I) (i.e. a stronger $dM \rightarrow \pi^a CO_{II}$ interaction than the $dM \rightarrow \pi^a CO_I$ interaction) (Tables 2,13). This is indicative of a stronger $M{-}CO_{II}$ than $M{-}CO_I$ bond, and thus the $M{-}CO_{II}$ bond should be shorter than the $M{-}CO_I$ bond. In fact, for the $(CO)_4Mn\overset{H}{\underset{PPh_2}{\lessgtr}}Mn(CO)_4$, the $M{-}CO_I$ bonds (1.840Å) were found by X-ray diffraction studies to be much longer than the $M{-}CO_{II}$ bonds (1.788 Å) [5].

As was shown in Table 2, the charges on CO_I groups and the overlap population $M{-}CO_I$ change only very little with replacement of one of the bridge hydrogen atom by the ligand L. However, for anions with a mixed bridge there is an additional difference in the negative charge on the CO_{II} carbonyl in *cis* ($CO_{II}{}^c$) and

Table 10

Energies and compositions of highest occupied molecular energy levels of $(\mathrm{CO})_4\mathrm{Mn}\genfrac{}{}{0pt}{}{\mathrm{H}}{\mathrm{PH}_2}\mathrm{Mn}(\mathrm{CO})_4$ with C_{2v} symmetry, calculation including $3d$ AO's of P atom

MO	Energy (eV)	Greatest contributions of the valence atomic orbitals (%)							
$18a_1$	−4.93	$p_y\mathrm{C_{II}}$	32	$d\mathrm{P}$	18	$p_y\mathrm{O_{II}}$	16	$s\mathrm{H_B}$	8
$16b_1$LUMO	−7.74	$3d_{z^2}\mathrm{Mn}$	20	$3d_{xz}\mathrm{Mn}$	13	$p_y\mathrm{C_{II}}$	10	$d\mathrm{P}$	8
$15b_1$HOMO	−11.93	$3d_{z^2}\mathrm{Mn}$	36	$p_y\mathrm{O_{II}}$	34	$3d_{x^2-y^2}\mathrm{Mn}$	10	$d\mathrm{P}$	4
$9a_2$	−11.96	$3d_{yz}\mathrm{Mn}$	46	$p_x\mathrm{O_{II}}$	18	$3d_{xy}\mathrm{Mn}$	15	$p_x\mathrm{C_{II}}$	3
$10b_2$	−12.27	$3d_{xy}\mathrm{Mn}$	43	$p_x\mathrm{O_{II}}$	22	$3d_{xz}\mathrm{Mn}$	13	$p_x\mathrm{O_I}$	8
$8a_2$	−12.78	$3d_{xy}\mathrm{Mn}$	39	$p_x\mathrm{O_{II}}$	19	$3d_{yz}\mathrm{Mn}$	15	$d\mathrm{P}$	8
$17a_1$	−12.79	$p_y\mathrm{O_{II}}$	38	$3d_{z^2}\mathrm{Mn}$	30	$3d_{x^2-y^2}\mathrm{Mn}$	11	$d\mathrm{P}$	8
$9b_2$	−13.33	$3d_{yz}\mathrm{Mn}$	37	$p_x\mathrm{O_{II}}$	21	$3d_{xy}\mathrm{Mn}$	11	$d\mathrm{P}$	10
$16a_1$	−14.77	$s\mathrm{H_B}$	48	$3d_{xz}\mathrm{Mn}$	14	$p_x\mathrm{Mn}$	12	$p_y\mathrm{O_{II}}$	10
$14b_1$	−15.08	$p_y\mathrm{O_{II}}$	35	$p_y\mathrm{P}$	19	$3d_{xz}\mathrm{Mn}$	15	$p_z\mathrm{Mn}$	7

Table 11

Energies and compositions of highest occupied molecular energy levels of $[(\mathrm{CO})_4\mathrm{Mo}\begin{smallmatrix}\mathrm{H}\\ \\ \mathrm{H}\end{smallmatrix}\mathrm{Mo}(\mathrm{CO})_4]^{-2}$ with D_{2h} symmetry, calculation excluding $5d$ AO's of Mo

MO	Energy (eV)	Greatest contributions of the valence atomic orbitals (%)							
$11a_g$	−0.69	$p_y\mathrm{O_I}$	31	$p_y\mathrm{C_I}$	60	$p_y\mathrm{C_{II}}$	3	$s\mathrm{H_B}$	3
$6b_{2g}$ LUMO	−1.96	$p_x\mathrm{O_I}$	45	$p_x\mathrm{C_I}$	35	$4d_{xz}\mathrm{Mo}$	20	$p_x\mathrm{Mo}$	10
$10a_g$ HOMO	−4.19	$p_y\mathrm{O_{II}}$	50	$4d_{z^2}\mathrm{Mo}$	18	$p_y\mathrm{C_{II}}$	17	$4d_{x^2-y^2}\mathrm{Mo}$	13
$9b_{1u}$	−4.23	$p_y\mathrm{O_{II}}$	45	$4d_{z^2}\mathrm{Mo}$	20	$p_y\mathrm{C_{II}}$	17	$4d_{x^2-y^2}\mathrm{Mo}$	14
$6b_{3g}$	−4.47	$4d_{yz}\mathrm{Mo}$	35	$p_y\mathrm{O_I}$	29	$p_x\mathrm{O_{II}}$	17	$p_y\mathrm{C_I}$	11
$3a_u$	−4.73	$4d_{xy}\mathrm{Mo}$	33	$p_x\mathrm{O_I}$	30	$p_x\mathrm{O_{II}}$	21	$p_x\mathrm{C_I}$	11
$6b_{2u}$	−4.74	$p_y\mathrm{O_I}$	34	$4d_{yz}\mathrm{Mo}$	32	$p_x\mathrm{O_{II}}$	16	$p_y\mathrm{C_I}$	13
$3b_{1g}$	−4.75	$4d_{xy}\mathrm{Mo}$	32	$p_x\mathrm{O_I}$	31	$p_x\mathrm{O_{II}}$	21	$p_x\mathrm{C_I}$	12
$6b_{3u}$	−6.48	$s\mathrm{H_B}$	54	$p_x\mathrm{Mo}$	16	$p_x\mathrm{O_I}$	8	$4d_{xz}\mathrm{Mo}$	8
$9a_g$	−8.07	$s\mathrm{H_B}$	54	$p_y\mathrm{O_I}$	15	$p_z\mathrm{Mo}$	12	$4d_{z^2}\mathrm{Mo}$	6
$5b_{3g}$	−8.09	$p_x\mathrm{O_{II}}$	55	$p_x\mathrm{C_{II}}$	17	$p_y\mathrm{O_I}$	17	$p_y\mathrm{Mo}$	2

Table 12

Energies and compositions of highest occupied molecular energy levels of $[(\mathrm{CO})_4\mathrm{Mo}\overset{\mathrm{H}}{\underset{\mathrm{PH}_2}{\lessgtr}}\mathrm{Mo}(\mathrm{CO})_4]^{-2}$ calculation including 3*d* AO's of P and without use of the 5 AO's of Mo (C_{2v} symmetry)

MO	Energy (eV)	Greatest contributions of the valence atomic orbitals (%)							
$18a_1$	−0.71	p_yC_I	57	p_yO_I	29	dP	3	sH_B	2
$16b_1$ LUMO	−1.06	p_yC_I	28	p_xC_I	20	p_yO_I	16	dP	2
$15b_1$ HOMO	−4.23	p_yO_{II}	38	$4d_{z^2}$Mo	23	p_yC_{II}	17	dP	4
$9a_2$	−4.43	$4d_{yz}$Mo	22	p_xO_{II}	18	p_yO_I	18	$4d_{xy}$Mo	10
$10b_2$	−4.57	p_xO_I	24	$4d_{xy}$Mo	23	p_xO_{II}	16	p_xC_{II}	9
$17a_1$	−4.62	p_yO_{II}	38	$4d_{z^2}$Mo	20	$4d_{x^2-y^2}$Mo	12	dP	6
$8a_2$	−4.91	$4d_{xy}$Mo	22	p_xO_I	19	p_xO_{II}	16	dP	7
$9b_2$	−5.31	$4d_{yz}$Mo	23	p_yO_I	22	p_xO_{II}	13	dP	11
$16a_1$	−6.73	sH_B	38	p_xMo	14	$4d_{xz}$Mo	9	dP	7
$14b_1$	−7.62	p_yO_{II}	26	p_yP	21	p_xO_I	13	$4d_{xz}$Mo	3

trans ($CO_{II}{}^{t}$) positions relative to the bridge hydrogen atom. The decrease of charge on the $CO_{II}{}^{t}$ group compared with the charge on the $CO_{II}{}^{c}$ group (as a result of the weaker $dM \rightarrow \pi^{a}CO_{II}{}^{t}$ interaction than the $dM \rightarrow \pi^{a}CO_{II}{}^{c}$ interaction and leading to elongation of the $M{-}CO_{II}{}^{t}$ bond compared with $M{-}CO_{II}{}^{c}$ bond) is indicative of a more powerful *trans* effect of the H^- bridge ligand compared with the *trans* effect of the OH^-, Cl^-, or $PH_2{}^-$ bridge ligand.

In conclusion the greater the difference in charges of $CO_{II}{}^{c}$ and $CO_{II}{}^{t}$ groups, the

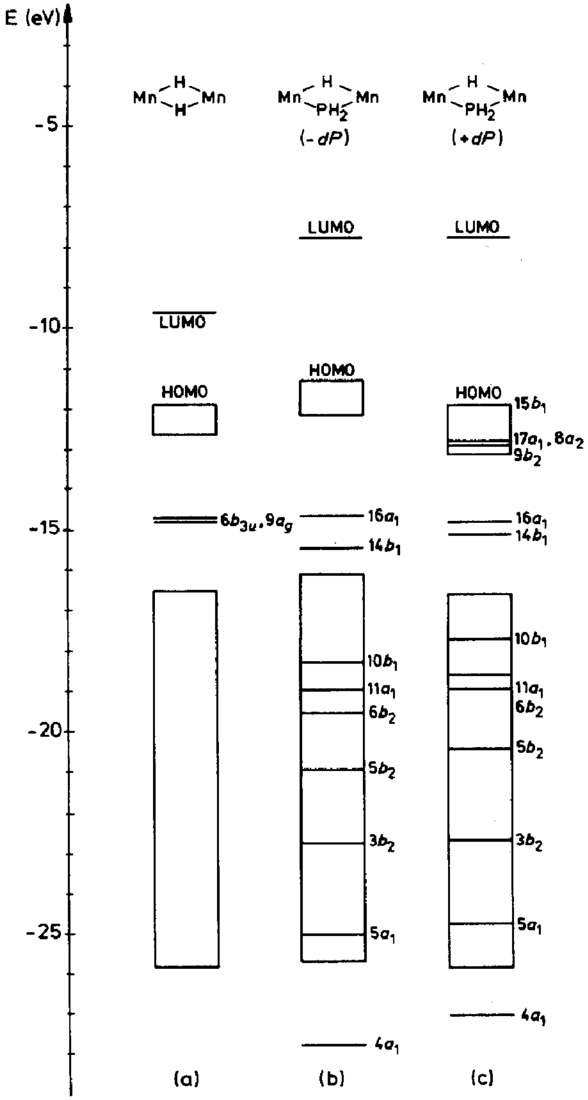

Fig. 5. Electronic structure of the carbonyl dimers of Mn showing all bridge levels for: (a) $(CO)_4Mn\genfrac{}{}{0pt}{}{H}{H}Mn(CO)_4$, (b) $(CO)_4Mn\genfrac{}{}{0pt}{}{H}{PH_2}Mn(CO)_4$ calculation excluding the 3*d* AO's of P atom, (c) $(CO)_4Mn\genfrac{}{}{0pt}{}{H}{PH_2}Mn(CO)_4$ calculation including the 3*d* AO's of P atom

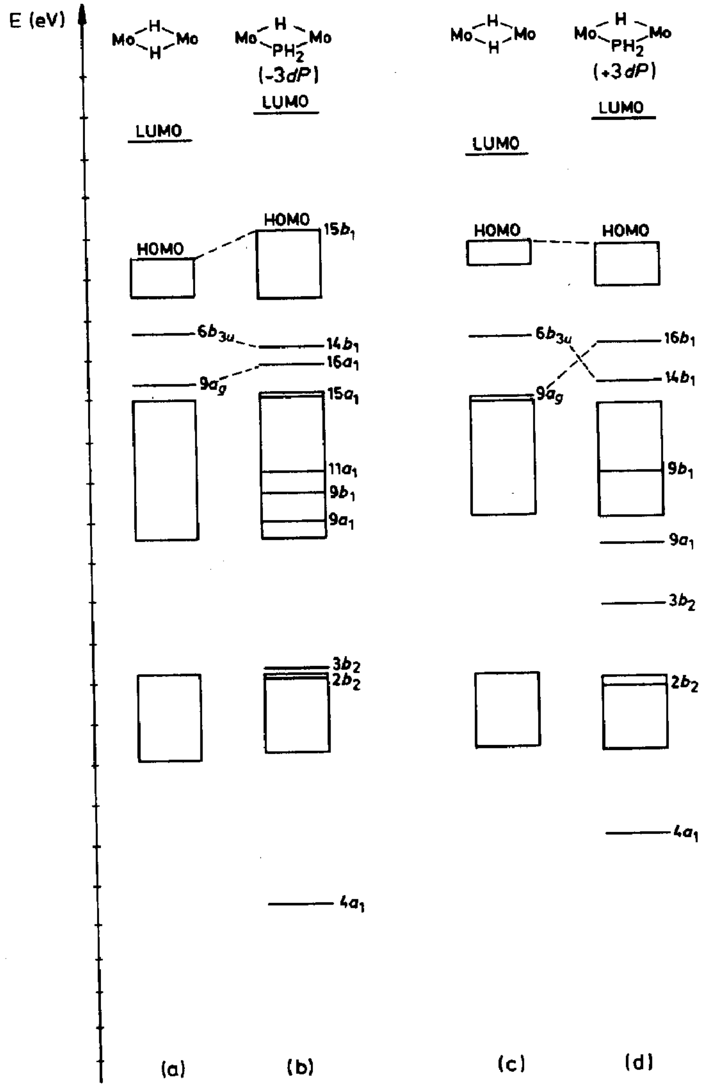

Fig. 6. Electronic structure of the carbonyl dimers of Mo showing all bridge levels for: (a) $[(CO)_4Mo\underset{H}{\overset{H}{<>}}Mo(CO)_4]^{-2}$ calculation including the 5*d* AO's of Mo atoms, (b) $[(CO)_4Mo\underset{PH_2}{\overset{H}{<>}}Mo(CO)_4]^{-2}$ calculation including the 5*d* AO's of Mo and excluding the 3*d* AO's of P atom, (c) $[(CO)_4Mo\underset{H}{\overset{H}{<>}}Mo(CO)_4]^{-2}$ calculation excluding the 5*d* AO's of Mo atoms (d) $[(CO)_4Mo\underset{PH_2}{\overset{H}{<>}}Mo(CO)_4]^{-2}$ calculation excluding the 5*d* AO's of Mo atoms and including the 3*d* AO's of P atom.

stronger is the *trans* effect of the bridge ligand H^- compared with that of the bridge ligand L; the change in the *trans* effect characteristic for the $[(CO)_4Mo\underset{L}{\overset{H}{<>}}Mo(CO_4)]^{-2}$ anions studied falls in the order: $H^- > PH_2^- > OH^- > Cl^-$ (Table 14).

Table 13

Mulliken atomic charges and overlap populations for $(CO)_4Mn\genfrac{\langle}{\rangle}{0pt}{}{H}{H}Mn(CO)_4$ and $(CO)_4Mn\genfrac{\langle}{\rangle}{0pt}{}{H}{PH_2}Mn(CO)_4$

Charges and overlap populations	Calculation excluding 4*d* AO's of Mn		
	$(CO)_4Mn\genfrac{\langle}{\rangle}{0pt}{}{H}{H}Mn(CO)_4$	$(CO)_4Mn\genfrac{\langle}{\rangle}{0pt}{}{H}{PH_2}Mn(CO)_4$ Calculation excluding 3*d* AO's of P	$(CO)_4Mn\genfrac{\langle}{\rangle}{0pt}{}{H}{PH_2}Mn(CO)_4$ Calculation including 3*d* AO's of P
Mn	−0.060	−0.509	−0.280
H_B	−0.178	−0.146	−0.143
L_B		PH_2 0.553	PH_2 −0.004
		P 0.945	P 0.212
		H −0.196	H −0.108
CO_{II} [a]	−0.058	−0.052 [c]	−0.034 [c]
		−0.032 [t]	−0.014 [t]
CO_I	0.177	0.195	0.201
Mn–Mn	0.032	−0.048	−0.053
Mn–H_B	0.141	0.141	0.131
Mn–L_B	0.141	0.255	0.434
Mn–CO_{II} [b]	0.421	0.445 [c]	0.409 [c]
		0.425 [t]	0.365 [t]
Mn–CO_I	0.397	0.406	0.393
*d*Mn–CO_{II}	0.237	0.234 [c]	0.226 [c]
		0.219 [t]	0.200 [t]
*d*Mn–CO_I	0.190	0.184	0.184

[a,b] *c* values are related to carbonyl groups in the *cis* position to bridge hydrogen atom($CO_{II}{}^{c}$) *t* values are related to carbonyl groups in the *trans* position to bridge hydrogen atom($CO_{II}{}^{t}$)

Table 14

Trans effect of the bridge ligand L

Bridge cores	The difference between charges of $CO_{II}{}^{c}$ and $CO_{II}{}^{t}$ groups, $\lvert Q_{CO_{II}{}^{c}} - Q_{CO_{II}{}^{t}} \rvert$
$Mo\genfrac{\langle}{\rangle}{0pt}{}{H}{H}Mo$	0.000
$Mo\genfrac{\langle}{\rangle}{0pt}{}{H}{PH_2}Mo$	0.039 (calculation excluding 3*d* AO's of P)
	0.012 (calculation including 3*d* AO's of P)
$Mo\genfrac{\langle}{\rangle}{0pt}{}{H}{OH}Mo$	0.040
$Mo\genfrac{\langle}{\rangle}{0pt}{}{H}{Cl}Mo$	0.066

Conclusions

We have found that in complexes of the type $[(CO)_4Mo\genfrac{\langle}{\rangle}{0pt}{}{H}{L}Mo(CO)_4]^{-2}$, where $L = H^-$, OH^-, Cl^-, $PH_2{}^-$ the bridge ligands L play almost the same role. The exchange one of the hydrogen bridge atoms by the ligand L does not cause significant rearrangement of the molecular levels. The energy of the HOMO level is very similar for all these complexes except for that of $[(CO)_4Mo\overset{H}{\underset{PH_2}{<>}}Mo(CO)_4]^{-2}$ if the $3d$ AO's of the P atom are excluded in the calculation.

If the atomic base used in the calculations did have these atomic orbitals, the HOMO level in $[(CO)_4Mo\overset{H}{\underset{PH_2}{<>}}Mo(CO)_4]^{-2}$ would have been stabilized and its energy would have approached the values for dimers having double hydrogen bridges and double mixed bridges, where $L = OH^-$, Cl^-. The results are similar for $(CO)_4Mn\overset{H}{\underset{PH_2}{<>}}Mn(CO)_4$. In conclusion the $3d$ AO's of P cause the stabilization of the highest occupied energy levels.

Similar to previously reported studies of the complexes with triple mixed bridges we now state that on going from $[(CO)_4M\overset{H}{\underset{H}{<>}}M(CO)_4]^n$ to $[(CO)_4M\overset{H}{\underset{L}{<>}}M(CO)_4]^n$ some of the molecular levels corresponding to the M–L–M bridge bond have the same energy as the molecular levels that correspond to the M–H–M bond that it replaces. On the other hand the AO's of the L bridge ligands are more delocalized and therefore the stability of the M–L–M bridge bond would be greater than that of the M–H–M bridge bond. The characters of the M–H–M and M–L–M bonds in the $[(CO)_4M\overset{H}{\underset{L}{<>}}M(CO)_4]^n$ are similar and are linked to metal type. For the molybdenum dimer these bonds are partly ionic because of positively charged metal atoms and the negatively charged bridge ligands. We stress that the charges of H, OH and Cl are very close. In the case of the $[(CO)_4Mo\overset{H}{\underset{PH_2}{<>}}Mo(CO)_4]^{-2}$ the negative charge of PH_2 is much lower than the negative charge of H if we disregard the participation of the $3d$ AO's of the P in the make up of the Mo–PH_2–Mo bond. However, if the acceptor character of the PH_2 group is also taken into account then its negative charge is very close to that of the H bridge atom.

The covalent character of the Mo–H–Mo, Mo–Cl–Mo and Mo–OH–Mo bonds is practically the same because of very close overlap populations: Mo–H, Mo–Cl, Mo–OH, but the covalent contribution to the Mo–PH_2–Mo bond is much greater because of the participation of the $3d$ AO's in making up that bond. The Mn–H–Mn and Mn–PH_2–Mn bonds have exclusively covalent character because the metal atoms and the bridge ligands are negatively charged. The covalent strength of the Mn–PH_2–Mn bridge bond is also much greater than that of the Mn–H–Mn bridge bond.

Thus, our calculations show that the participation of the $3d$ AO's of the P atom in making up the M–PH_2–M bridge bond, is the same as that which we described previously for the terminal M–PH_3 bonds [9].

We have also showed that the *trans* effect of the H^- bridge ligand is a little higher than the *trans* effect of other bridge ligands L such as Cl^-, OH^-, PH_2^-. Recently we reported similar conclusions for H^-, Cl^-, CO bridge ligands in the complexes $[L_3M\overset{H}{\underset{L}{<L>}}ML_3]^n$ [2].

Acknowledgement

This work was supported financially by Project No. CPBP 01.12 of the Polish Academy of Sciences.

References

1 R. Bau, P. Gütlich and R.G. Teller, Structure and Bonding, 44 (1981) 3.

2 B. Jeżowska-Trzebiatowska and B. Nissen-Sobocińska, J. Organomet. Chem., 342 (1988) 353.

3 B. Jeżowska-Trzebiatowska and B. Nissen-Sobocińska, J. Organomet. Chem., 342 (1988) 215.

4 (a) J.L. Petersen and J.M. Williams, Inorg. Chem., 17 (1978) 1308. (b) J.L. Petersen, L.F. Dahl and J.M. Williams, J. Am. Chem. Soc., 96 (1974) 6610. (c) R.J. Doedens and L.F. Dahl, J. Am. Chem. Soc., 87 (1965) 2576.

5 R.J. Doedens, W.T. Robinson and J.A. Ibers, J. Am. Chem. Soc., (1967) 4323.

6 A. Bino and F.A. Cotton, J. Am. Chem. Soc., 101 (1979) 4150.

7 N.J. Cooper, M.L.H. Green, C. Couldwell and K. Prout, J. Chem. Soc., Chem. Comm., (1978) 145.

8 M.B. Hall and R.F. Fenske, Inorg. Chem., 11 (1972) 768.

9 B. Jeżowska-Trzebiatowska and B. Nissen-Sobocińska, J. Organomet. Chem., 369 (1989) 69.